

Anisotropy Scaling Functions in Heavy-Ion Collisions: Insights into the ‘Ultra-Central Flow Puzzle’ and Constraints on Transport Coefficients and Nuclear Deformation

Roy A. Lacey^{1,*}

¹Department of Chemistry, Stony Brook University,
Stony Brook, NY, 11794-3400, USA

(Dated: May 3, 2024)

Anisotropy scaling functions derived from comprehensive measurements of transverse momentum- and centrality-dependent anisotropy coefficients $v_2(p_T, \text{cent})$ and $v_3(p_T, \text{cent})$ in Pb+Pb collisions at 5.02 and 2.76 TeV, and Xe+Xe collisions at 5.44 TeV at the LHC, offer new insights into the ‘ultra-central flow puzzle’. These functions integrate diverse measurements into a single curve, clarifying anisotropy attenuation throughout the entire p_T and centrality range. They reveal the influence of initial-state eccentricities (ε_n), dimensionless size (\mathbb{R}), radial flow, viscous correction to the thermal distribution function (δ_f), the medium’s stopping power (\hat{q}), and specific shear viscosity (η/s) on the observed anisotropies. This analysis not only enhances understanding of transport coefficients but also provides crucial constraints on nuclear deformation.

PACS numbers: 25.75.-q, 25.75.Dw, 25.75.Ld

Azimuthal anisotropy measurements are pivotal in the study of the quark-gluon plasma (QGP) produced in heavy ion collisions at the Relativistic Heavy Ion Collider (RHIC) and the Large Hadron Collider (LHC). These measurements, crucial for determining the temperature (T) and baryon chemical potential (μ_B) dependence of transport coefficients, are quantified by the complex coefficients [1–3]:

$$V_n \equiv v_n e^{in\Psi_n} = \langle e^{in\phi} \rangle, \quad (1)$$

where v_n represents the degree of azimuthal anisotropy, Ψ_n is the event-plane angle, and $\langle \cdot \rangle$ denotes averaging over the single-particle spectrum within an event.

These v_n values are linked to the Fourier coefficients v_{nn} , which describe the intensity of two-particle correlations in azimuthal angle differences $\Delta\phi = \phi_i - \phi_j$ [4, 5]:

$$\frac{dN_{\text{pairs}}}{d\Delta\phi} \propto 1 + 2 \sum_{n=1}^{\infty} v_{nn} \cos(n\Delta\phi), \quad (2)$$

$$v_{nn}(p_T^i, p_T^j) = v_n(p_T^i)v_n(p_T^j) + \delta_{\text{NF}},$$

where δ_{NF} indicates non-flow contributions, minimized through specific experimental methodologies [5–8].

The coefficients v_n are fundamentally linked to collective flow dynamics for $p_T \lesssim 4\text{--}5 \text{ GeV}$, transitioning to jet quenching at higher p_T . This behavior is supported by extensive research [9–41], which highlights the impact of radial expansion, v_n -fluctuations, p_T -dependent viscous attenuation, jet quenching, and initial-state anisotropy on v_n . The transverse plane density profile $\rho(r, \varphi)$ is quantified by complex eccentricity coefficients:

$$\mathcal{E}_n \equiv \varepsilon_n e^{in\Phi_n} = \frac{\int d^2 r_\perp r^m e^{in\varphi} \rho(r, \varphi)}{\int d^2 r_\perp r^m \rho(r, \varphi)}, \quad (3)$$

where r and φ represent the radius and azimuthal angle, respectively, and Φ_n denotes the angle of the n^{th} -order participant plane ($m = n$ for $n \geq 2$ and $m = 3$ for $n = 1$) [17, 22, 42,

43]. The deformed Woods-Saxon distribution, employed to model nucleon configurations in non-spherical nuclei, is described by:

$$\rho(r, \theta, \varphi) = \frac{\rho_0}{1 + \exp\left(\frac{r-R(\theta, \varphi)}{a}\right)}, \quad (4)$$

$$R(\theta, \varphi) = R_0 \{1 + \beta_2 [\cos \gamma Y_{20}(\theta, \varphi) + \sin \gamma Y_{22}(\theta, \varphi)]\},$$

where ρ_0 is the central density, R_0 the nuclear radius, and a the skin thickness. The spherical harmonics Y_{lm} , along with coefficients β_2 and γ , shape the nucleus, with β_2 measuring deformation magnitude and γ indicating asymmetry degrees between 0 and 60°. Fluctuations in the initial state density profile lead to variations in ε_n .

Dynamical models based on relativistic hydrodynamics, which suggest a roughly linear relationship $v_n \propto \varepsilon_n$ [43–45], have successfully replicated the observed magnitudes and trends of v_n coefficients [15, 22, 32, 46–49]. These models are also central to efforts employing Bayesian inference to constrain the transport properties of the QGP [50–57]. However, they encounter significant challenges in ultra-central collisions (cent $\lesssim 1\%$), where they struggle to simultaneously predict v_2 and v_3 accurately [58]. Typically, these models either overestimate v_2 or underestimate v_3 , or display both discrepancies.

The inability of hydrodynamic models to accurately describe both v_2 and v_3 in ultra-central collisions presents a significant challenge, contradicting the expectations set for these collisions. Conventionally, models were expected to perform well in central collisions due to higher charge particle multiplicities $\langle N_{\text{chg}} \rangle$ and larger volumes of locally thermalized domains. This discrepancy raises doubts about whether these widely used models are missing crucial components necessary for accurately depicting the initial state and transport coefficients.

Despite extensive efforts to resolve the ‘ultra-central flow puzzle’ by refining initial conditions [59–68], examining transport coefficients [59, 61, 69, 70], and evaluating equa-

tions of state [71], a definitive resolution remains elusive. The ongoing investigations highlight the complexity of accurately modeling these critical aspects of QGP behavior.

In this study, we develop anisotropy scaling functions, premised on the idea that diverse measurements of $v_2(p_T, \text{cent})$ and $v_3(p_T, \text{cent})$ can be unified into a single, coherent scaling function. This unification integrates various parameters affecting $v_n(p_T, \text{cent})$, including initial-state eccentricities (ε_n), dimensionless size ($\mathbb{R} \propto RT$), radial flow magnitude, the medium's stopping power (\hat{q}), and the specific shear viscosity or viscosity-to-entropy ratio ($\eta/s \propto T^3/\hat{q}$), along with the viscous correction to the thermal distribution function (δ_f) [13, 72].

These parameters contribute to the expression of the anisotropy coefficients, which can be described by Eq. 5 [35, 73–75]:

$$v_n(p_T, \text{cent}) = \varepsilon_n e^{-\frac{\beta}{\mathbb{R}}[n(n+\kappa p_T^2)]}, \quad n = 2, 3, \quad (5)$$

where $\beta \propto \eta/s$, $\delta_f = \kappa p_T^2$ [13, 35], and $\mathbb{R} \propto \langle N_{\text{chg}} \rangle_{|\eta| \leq 0.5}^{1/3}$ is related to the mid-rapidity ($|\eta| \leq 0.5$) charged particle multiplicity. The transition from flow to jet quenching at higher p_T is managed by maintaining consistency between η/s and \hat{q} , ensuring a smooth transition in the low and high momentum regions of δ_f . This shift is facilitated by fixing the κp_T^2 term in Eq. 5 to remain constant for p_T values above approximately 4.5 GeV/c, marking the threshold between flow-dominated and jet-quenching domains.

Equation 5 reveals a crucial insight: In the domain of the most central collisions, characterized by the peak value \mathbb{R}_0 , a scaling connection emerges. This equation links the observed values of the harmonic $v_n(p_T, 0)$ in these ultra-central events with those observed as $v'_n(p_T, \text{cent})$ at different centralities, each tied to its corresponding \mathbb{R}' value:

$$\frac{v_n(p_T, 0)}{v_n(0)} e^{\frac{n\beta}{\mathbb{R}_0}(n+\kappa p_T^2)} = \left(\frac{v'_n(p_T, \text{cent})}{v'_n(\text{cent})} \right) e^{\frac{n\beta}{\mathbb{R}'_0}(n+\kappa p_T^2)(\frac{\mathbb{R}_0}{\mathbb{R}'} - 1)}, \quad (6)$$

where the exponential on the left-hand side of the equation accounts for the anisotropy attenuation in ultra-central collisions, and that on the right-hand side accounts for the relative attenuation at other centralities.

Moreover, when preserving a fixed centrality within a given system, a revealing correlation emerges between the values of $v_2(p_T, \text{cent})$ and $v_3(p_T, \text{cent})$. These values, both subject to the same influences of radial flow, η/s , and \hat{q} , adhere to the following relationship:

$$\frac{v_2(p_T, \text{cent})}{v_2(\text{cent})} e^{\frac{2\alpha\beta}{\mathbb{R}_0}} = \left(\frac{v_3(p_T, \text{cent})}{v_3(\text{cent})} \right)^{\frac{2}{3}}, \quad (7)$$

where α represents a system-dependent (yet centrality-independent) normalizing constant. Equations 6 and 7 encapsulate the intricate dependencies of the high and low p_T anisotropy coefficients from ultra-central to peripheral collisions, underlining that the scaled values of $v_2(p_T, \text{cent})$ and $v_3(p_T, \text{cent})$ measurements can be effectively collapsed onto a

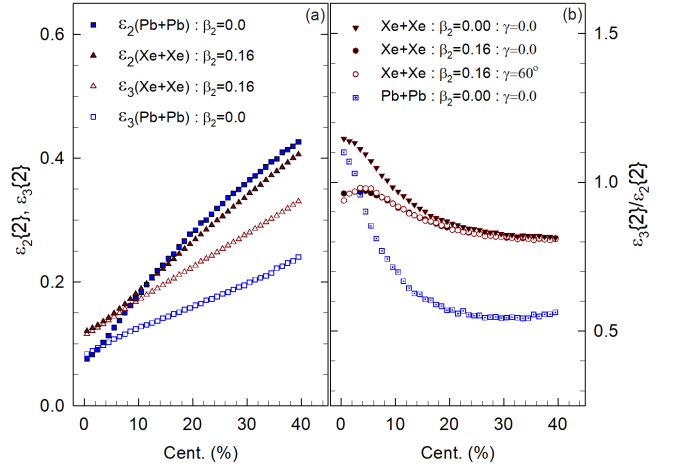


FIG. 1. (Color Online) Panel (a) contrasts the centrality-dependent values of $\varepsilon_2(\text{cent})$ and $\varepsilon_3(\text{cent})$ for 5.02 TeV Pb+Pb collisions featuring spherical Pb nuclei and 5.44 TeV Xe+Xe collisions for deformed Xe nuclei. In panel (b), the ratios $\varepsilon_3(\text{cent})/\varepsilon_2(\text{cent})$ are compared for spherical Pb nuclei ($\beta_2 = 0$) and both spherical and deformed Xe nuclei (cf. Eq. 4), as indicated.

single curve or scaling function S_{FS} . Therefore, the identification of such a scaling function would furnish compelling evidence for the coherence of the scaling coefficients and the trustworthiness of the corresponding eccentricity spectrum and its ratios.

The eccentricity ratio, as shown in Fig. 1, is crucial for understanding the nuanced impact of centrality and deformation on collision dynamics. This figure displays the calculated values of $\varepsilon_2(\text{cent})$, $\varepsilon_3(\text{cent})$, and their ratios for Pb+Pb and Xe+Xe collisions at 5.02 TeV and 5.44 TeV. These values reveal distinct dependencies that not only help refine the eccentricity spectrum but also illuminate the initial-state deformation of the Xe nucleus. Particularly in ultra-central and central collisions, these measurements are vital for accurately quantifying nuclear deformation. Additionally, the ratio $\varepsilon_2(\text{cent})/\varepsilon_3(\text{cent})$ demonstrates insensitivity to variations in γ , highlighting its stability across different asymmetries.

The data utilized in this study are sourced from the ATLAS [8, 76] and ALICE [77, 78] collaborations, encompassing $v_2(p_T, \text{cent})$ and $v_3(p_T, \text{cent})$ measurements for Pb+Pb collisions at $\sqrt{s_{\text{NN}}} = 2.76$ and 5.02 TeV, as well as Xe+Xe collisions at 5.44 TeV. The required centrality-dependent $\langle N_{\text{chg}} \rangle_{|\eta| \leq 0.5}$ values were derived from corresponding multiplicity density measurements [79–82]. We adopted the previously established value $\kappa = 0.17 (\text{GeV}/c)^{-2}$ [35] to compute δ_f . The eccentricities were computed according to the procedure outlined in Eq. 3, with the assistance of a Monte Carlo quark-Glauber model (MC-qGlauber) featuring fluctuating initial conditions [35]. This model, based on the widely used MC-Glauber model [83, 84], accounts for the finite size of the nucleon, the nucleon's wounding profile, the distribution of quarks within the nucleon, and quark cross sections

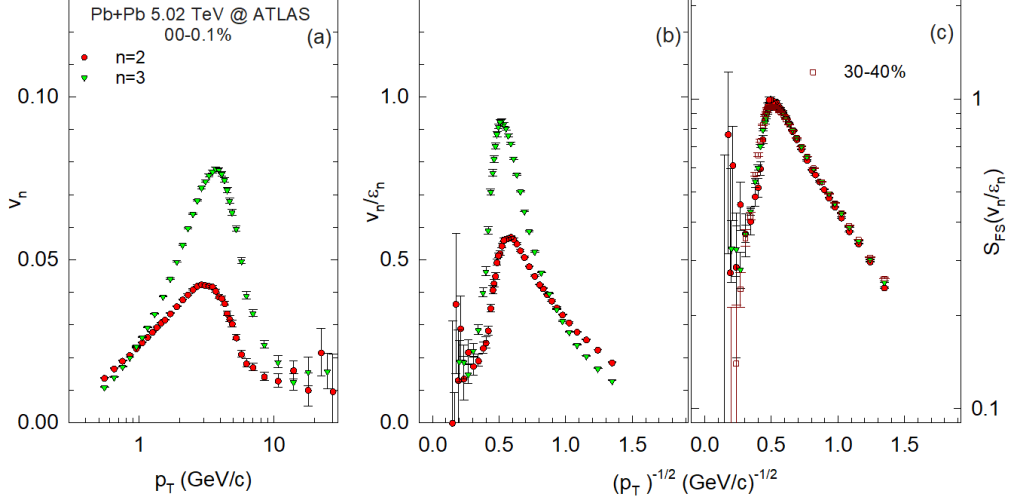


FIG. 2. (Color Online) Comparison of $v_2(p_T)$ and $v_3(p_T)$ in panel (a), their eccentricity-scaled values v_2/ε_2 and v_3/ε_3 in panel (b), and the resulting scaling function in panel (c) for 0.1% central Pb+Pb collisions at 5.02 TeV. Panel (c) also includes scaled results for 30-40% central Pb+Pb collisions. The data are sourced from the ATLAS collaboration [76].

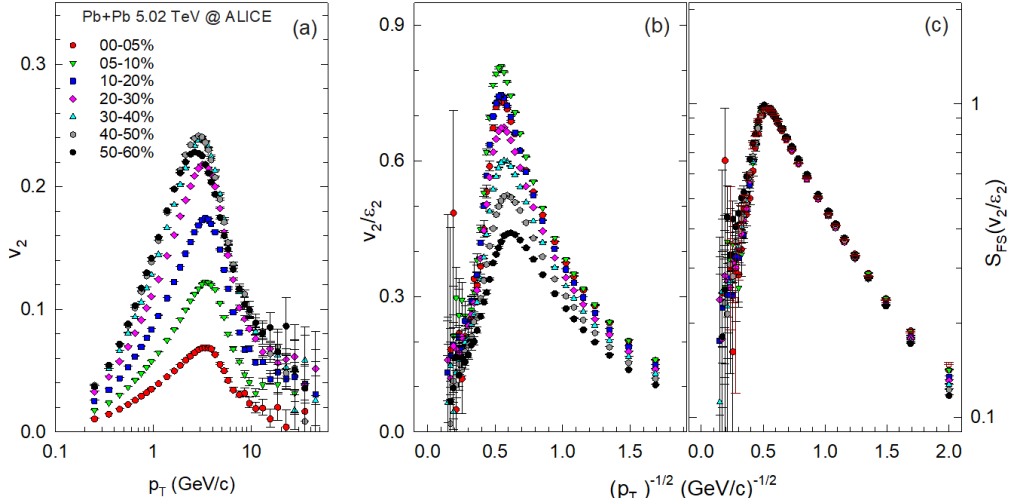


FIG. 3. (Color Online) Comparison of $v_2(p_T, \text{cent})$ in panel (a), their eccentricity-scaled values [$v_2(p_T, \text{cent})/\varepsilon_2(\text{cent})$] in panel (b), and the resulting scaling function in panel (c) for Pb+Pb collisions at 5.02 TeV. Data sourced from the ALICE collaboration [77].

that accurately reproduce the NN inelastic cross section for the corresponding beam energies. Calculations were performed for spherical Pb nuclei and Xe nuclei with varying degrees of initial-state deformation characterized with different values for the β_2 and γ parameters (cf. Eq. 4). A systematic uncertainty of 2-3% was estimated for the eccentricities based on variations in the model parameters.

The scaling functions were derived from differential measurements of $v_2(p_T, \text{cent})$ and $v_3(p_T, \text{cent})$ across a range of collision energies, including Pb+Pb collisions at 2.76 and 5.02 TeV, and Xe+Xe collisions at 5.44 TeV. This derivation utilized specific equations (6 and 7), with the reference value \mathbb{R}_0 for ultra-central Pb+Pb collisions at 5.02 TeV. In Figure 2,

we illustrate the scaling procedure for 0.1% central Pb+Pb collisions at 5.02 TeV, employing $1/\sqrt{p_T}$ for the x-axis in panels (b) and (c) to highlight the flow- and jet-quenching-dominated domains. Panel (a) emphasizes the discrepancy between $v_2(p_T)$ and $v_3(p_T)$, while panel (b) shows that eccentricity scaling alone ($v_2(p_T)/\varepsilon_2$ and $v_3(p_T)/\varepsilon_3$) fails to capture their difference. Panel (c) showcases the resulting scaling function, indicating convergence of data onto a single curve for both p_T domains, providing robust evidence for the consistency of the scaling coefficients and the validity of the corresponding eccentricity spectrum and its ratios. Validation of the scaling function spanned the entire measurement range (0.0-0.1% to 50-60%) for specific parameters ($\beta = 0.88$ and

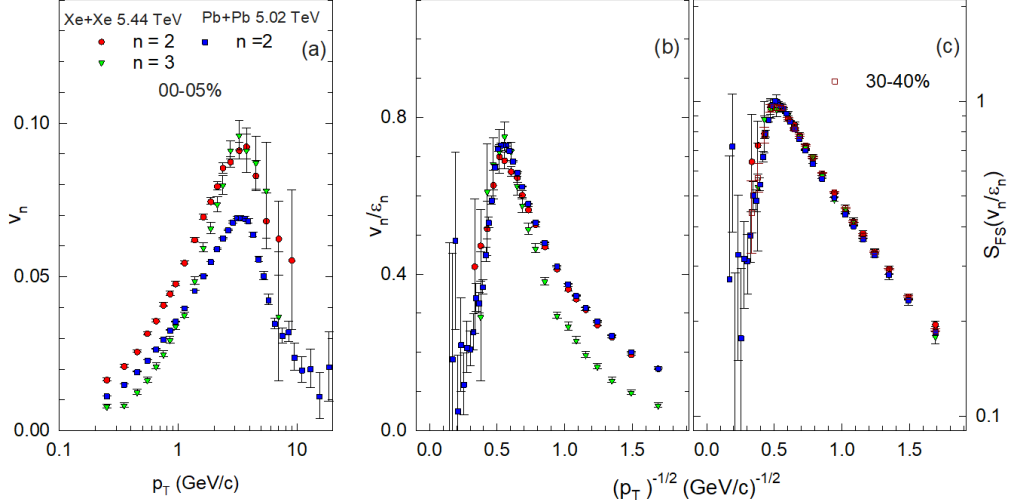


FIG. 4. (Color Online) Comparison of the $v_2(p_T, \text{cent})$ and $v_3(p_T, \text{cent})$ values for Xe+Xe collisions and $v_2(p_T, \text{cent})$ for Pb+Pb collisions in panel (a), their eccentricity-scaled values $v_2(p_T, \text{cent})/\varepsilon_2(\text{cent})$ and $v_3(p_T, \text{cent})/\varepsilon_3(\text{cent})$ in panel (b), and the resulting scaling function in panel (c) for 0-5% central collisions. Panel (c) also includes scaled results for 30-40% central Xe+Xe collisions. The data are sourced from the ALICE collaboration [77, 78].

$\alpha = 1$), as demonstrated in Figure 3 for $v_2(p_T, \text{cent})$ measurements. The attenuation factor for the 0-5% centrality cut reflects an average incorporating values from both ultra-central and non-ultra-central collisions, considering contributions from both scenarios.

A similarly robust scaling function, closely matching that for Pb+Pb collisions at 5.02 TeV, was obtained across the full range of measurements for Pb+Pb collisions at 2.76 TeV. Characterized by scaling exponents $\beta = 0.84$ and $\alpha = 1.25$, the results indicate an approximate 5% reduction in η/s when the collision energy decreases from 5.02 TeV to 2.76 TeV. Importantly, the consistency of the scaling functions at both energies suggests a negligible influence from non-flow effects.

The observed scaling function, consistent across both flow and jet-quenching domains with identical scaling coefficients, not only constrains η/s and \hat{q} but also supports the relationship between η/s and T^3/\hat{q} proposed by Majumder et al. [72]. This scaling, notably the high p_T anisotropy's dependence on the dimensionless size $\mathbb{R} \propto \langle N_{\text{chg}} \rangle^{1/3}$, underscores the influence of path length and highlights the role of radiative energy loss in shaping jet-quenching-induced anisotropy. Moreover, the seamless transition observed between the low and high momentum regions at the p_T threshold, which delineates flow from jet-quenching domains, provides crucial insights into the relative magnitude of η/s and T^3/\hat{q} [13]. This distinction is critical for identifying the nature of the quark-gluon plasma as either strongly or weakly coupled. A preliminary analysis, following the δf formalism in Ref. [13] and reconciling η/s with \hat{q} , suggests that η/s exceeds T^3/\hat{q} , indicating a strongly coupled plasma.

The scaling function elucidates nuclear deformation, as illustrated in Figs. 1 and 4. In Fig. 4, we compare $v_2(p_T)$ and

$v_3(p_T)$ from Xe+Xe collisions against $v_2(p_T)$ from Pb+Pb collisions at 0-5% centrality, using eccentricities for the deformed Xe nucleus ($\beta_2 = 0.16$ [85]). Panel (a) highlights significant differences in viscous attenuation between these harmonics, with Xe+Xe showing larger magnitudes, aligned with its higher eccentricities (cf. Fig. 1). Panel (b) acknowledges that eccentricity scaling does not entirely account for these differences but clarifies the contrast in $v_2(p_T)$ between Xe and Pb. Panel (c) demonstrates the scaling function's ability to merge data into a single curve across both flow- and jet-quenching-dominated regimes, validating the consistency of scaling coefficients and the accuracy of the eccentricity spectrum for the deformed Xe nucleus. This spans centrality ranges from 0-5% to 40-50%, with $\beta = 0.90$, $\alpha = 0$, and $\beta_2 = 0.16$. Deviations from these values suggest mild deformations in Xe nuclei, correlating with an approximate 2% increase in η/s when increasing the collision energy from 5.02 TeV to 5.44 TeV. Further analysis shows slightly higher radial flow in 5.02 TeV Pb+Pb collisions compared to 5.44 TeV Xe+Xe collisions.

The application of scaling functions to analyze nuclear deformation significantly enhances the precision of our studies. This method (i) compensates effectively for anisotropy attenuation in ultra-central collisions, (ii) decouples initial- and final-state effects, and (iii) relies on consistent measurements of $v_2(p_T)$ and $v_3(p_T)$ across events with identical η/s , multiplicity, and radial flow characteristics. Consequently, it markedly reduces systematic uncertainties.

In summary, anisotropy scaling functions, derived from extensive measurements of $v_2(p_T, \text{cent})$ and $v_3(p_T, \text{cent})$ in Pb+Pb collisions at 5.02 and 2.76 TeV, and Xe+Xe collisions at 5.44 TeV, provide crucial insights into the ‘ultra-central flow puzzle’ and constrain transport coefficients, the eccen-

tricity spectrum, and nucleus deformation. Consolidating diverse measurements into a single curve, these functions account for specific parameters influencing $v_n(p_T, \text{cent})$, including initial-state eccentricities (ε_n), dimensionless size (\mathbb{R}), radial flow magnitude, the medium's stopping power (\hat{q}), and its specific shear viscosity (η/s), as well as the viscous correction to the thermal distribution function (δ_f). They yield distinct constraints for transport coefficients and nucleus deformation.

ACKNOWLEDGEMENT

This research is supported by the US DOE under contract DE-FG02-87ER40331.A008.

* E-mail: Roy.Lacey@Stonybrook.edu

- [1] A. Bilandzic, R. Snellings, and S. Voloshin, *Phys. Rev.* **C83**, 044913 (2011), arXiv:1010.0233 [nucl-ex].
- [2] M. Luzum, *J. Phys.* **G38**, 124026 (2011), arXiv:1107.0592 [nucl-th].
- [3] D. Teaney and L. Yan, *Phys. Rev.* **C86**, 044908 (2012), arXiv:1206.1905 [nucl-th].
- [4] A. M. Poskanzer and S. A. Voloshin, *Phys. Rev.* **C58**, 1671 (1998), arXiv:nucl-ex/9805001 [nucl-ex].
- [5] R. A. Lacey, *Proceedings, 18th International Conference on Ultra-Relativistic Nucleus-Nucleus Collisions (Quark Matter 2005): Budapest, Hungary, August 4-9, 2005*, *Nucl. Phys.* **A774**, 199 (2006), arXiv:nucl-ex/0510029 [nucl-ex].
- [6] M. Luzum and J.-Y. Ollitrault, *Phys. Rev. Lett.* **106**, 102301 (2011), arXiv:1011.6361 [nucl-ex].
- [7] E. Retinskaya, M. Luzum, and J.-Y. Ollitrault, *Phys. Rev. Lett.* **108**, 252302 (2012), arXiv:1203.0931 [nucl-th].
- [8] G. Aad *et al.* (ATLAS), *Phys. Rev.* **C86**, 014907 (2012), arXiv:1203.3087 [hep-ex].
- [9] H. Song, S. A. Bass, U. Heinz, T. Hirano, and C. Shen, *Phys. Rev. Lett.* **106**, 192301 (2011), [Erratum: *Phys. Rev. Lett.* 109, 139904(2012)], arXiv:1011.2783 [nucl-th].
- [10] B. Alver *et al.* (PHOBOS), *Phys. Rev.* **C77**, 014906 (2008), arXiv:0711.3724 [nucl-ex].
- [11] B. Alver *et al.* (PHOBOS), *Phys. Rev.* **C81**, 034915 (2010), arXiv:1002.0534 [nucl-ex].
- [12] J.-Y. Ollitrault, A. M. Poskanzer, and S. A. Voloshin, *Phys. Rev. C* **80**, 014904 (2009), arXiv:0904.2315 [nucl-ex].
- [13] K. Dusling, G. D. Moore, and D. Teaney, *Phys. Rev.* **C81**, 034907 (2010), arXiv:0909.0754 [nucl-th].
- [14] R. A. Lacey, A. Tarantenko, R. Wei, N. Ajitanand, J. Alexander, *et al.*, *Phys. Rev.* **C82**, 034910 (2010), arXiv:1005.4979 [nucl-ex].
- [15] C. Shen, U. Heinz, P. Huovinen, and H. Song, *Phys. Rev. C* **84**, 044903 (2011), arXiv:1105.3226 [nucl-th].
- [16] H. Niemi, G. S. Denicol, H. Holopainen, and P. Huovinen, *Phys. Rev.* **C87**, 054901 (2013), arXiv:1212.1008 [nucl-th].
- [17] J. Fu, *Phys. Rev.* **C92**, 024904 (2015).
- [18] C. Andrés, J. Dias de Deus, A. Moscoso, C. Pajares, and C. A. Salgado, *EPJ Web Conf.* **90**, 08003 (2015).
- [19] M. Abdallah *et al.* (STAR), *Phys. Rev. Lett.* **129**, 252301 (2022), arXiv:2201.10365 [nucl-ex].
- [20] J. Adam *et al.* (STAR), *Phys. Lett.* **B783**, 459 (2018), arXiv:1803.03876 [nucl-ex].
- [21] J. Adam *et al.* (ALICE), *Phys. Rev. Lett.* **117**, 182301 (2016), arXiv:1604.07663 [nucl-ex].
- [22] Z. Qiu and U. W. Heinz, *Phys. Rev. C* **84**, 024911 (2011), arXiv:1104.0650 [nucl-th].
- [23] A. Adare *et al.* (PHENIX), *Phys. Rev. Lett.* **107**, 252301 (2011), arXiv:1105.3928 [nucl-ex].
- [24] N. Magdy (STAR), *Proceedings, 27th International Conference on Ultrarelativistic Nucleus-Nucleus Collisions (Quark Matter 2018): Venice, Italy, May 14-19, 2018*, *Nucl. Phys.* **A982**, 255 (2019), arXiv:1807.07638 [nucl-ex].
- [25] L. Adamczyk *et al.* (STAR), *Phys. Rev. C* **94**, 034908 (2016), arXiv:1601.07052 [nucl-ex].
- [26] L. Adamczyk *et al.* (STAR), *Phys. Rev. C* **93**, 014907 (2016), arXiv:1509.08397 [nucl-ex].
- [27] L. Adamczyk *et al.* (STAR), *Phys. Rev. Lett.* **115**, 222301 (2015).
- [28] L. Adamczyk *et al.* (STAR), *Phys. Rev. Lett.* **116**, 112302 (2016), arXiv:1601.01999 [nucl-ex].
- [29] J. Adam *et al.* (STAR), *Phys. Rev. Lett.* **122**, 172301 (2019), arXiv:1901.08155 [nucl-ex].
- [30] F. G. Gardim, J. Noronha-Hostler, M. Luzum, and F. Grassi, *Phys. Rev.* **C91**, 034902 (2015), arXiv:1411.2574 [nucl-th].
- [31] H. Holopainen, H. Niemi, and K. J. Eskola, *Phys. Rev.* **C83**, 034901 (2011), arXiv:1007.0368 [hep-ph].
- [32] G.-Y. Qin, H. Petersen, S. A. Bass, and B. Muller, *Phys. Rev. C* **82**, 064903 (2010), arXiv:1009.1847 [nucl-th].
- [33] C. Gale, S. Jeon, B. Schenke, P. Tribedy, and R. Venugopalan, *Phys. Rev. Lett.* **110**, 012302 (2013), arXiv:1209.6330 [nucl-th].
- [34] K. M. Burke *et al.* (JET), *Phys. Rev. C* **90**, 014909 (2014), arXiv:1312.5003 [nucl-th].
- [35] P. Liu and R. A. Lacey, *Phys. Rev. C* **98**, 021902 (2018), arXiv:1802.06595 [nucl-ex].
- [36] K. Adcox *et al.* (PHENIX), *Phys. Rev. Lett.* **88**, 022301 (2002), arXiv:nucl-ex/0109003.
- [37] C. Adler *et al.* (STAR), *Phys. Rev. Lett.* **89**, 202301 (2002), arXiv:nucl-ex/0206011.
- [38] H.-z. Zhang, J. F. Owens, E. Wang, and X. N. Wang, *J. Phys. G* **35**, 104067 (2008), arXiv:0804.2381 [hep-ph].
- [39] B. Abelev *et al.* (ALICE), *JHEP* **03**, 013 (2014), arXiv:1311.0633 [nucl-ex].
- [40] Y. Mehtar-Tani, J. G. Milhano, and K. Tywoniuk, *Int. J. Mod. Phys. A* **28**, 1340013 (2013), arXiv:1302.2579 [hep-ph].
- [41] G.-Y. Qin and X.-N. Wang, *Int. J. Mod. Phys. E* **24**, 1530014 (2015), arXiv:1511.00790 [hep-ph].
- [42] H. Niemi, K. J. Eskola, and R. Paatelainen, *Phys. Rev. C* **93**, 024907 (2016), arXiv:1505.02677 [hep-ph].
- [43] J. Noronha-Hostler, L. Yan, F. G. Gardim, and J.-Y. Ollitrault, *Phys. Rev. C* **93**, 014909 (2016), arXiv:1511.03896 [nucl-th].
- [44] M. D. Sievert and J. Noronha-Hostler, *Phys. Rev. C* **100**, 024904 (2019), arXiv:1901.01319 [nucl-th].
- [45] S. Rao, M. Sievert, and J. Noronha-Hostler, *Phys. Rev. C* **103**, 034910 (2021), arXiv:1910.03677 [nucl-th].
- [46] B. Schenke, S. Jeon, and C. Gale, *Phys. Lett. B* **702**, 59 (2011), arXiv:1102.0575 [hep-ph].
- [47] P. Bozek, *Phys. Rev. C* **85**, 034901 (2012), arXiv:1110.6742 [nucl-th].
- [48] F. G. Gardim, F. Grassi, M. Luzum, and J.-Y. Ollitrault, *Phys. Rev. Lett.* **109**, 202302 (2012), arXiv:1203.2882 [nucl-th].
- [49] T. Hirano, P. Huovinen, K. Murase, and Y. Nara, *Prog. Part. Nucl. Phys.* **70**, 108 (2013), arXiv:1204.5814 [nucl-th].

- [50] J. E. Bernhard, J. S. Moreland, S. A. Bass, J. Liu, and U. Heinz, *Phys. Rev. C* **94**, 024907 (2016), arXiv:1605.03954 [nucl-th].
- [51] J. E. Bernhard, J. S. Moreland, and S. A. Bass, *Nature Phys.* **15**, 1113 (2019).
- [52] J. S. Moreland, J. E. Bernhard, and S. A. Bass, *Phys. Rev. C* **101**, 024911 (2020), arXiv:1808.02106 [nucl-th].
- [53] D. Everett *et al.* (JETSCAPE), *Phys. Rev. Lett.* **126**, 242301 (2021), arXiv:2010.03928 [hep-ph].
- [54] D. Everett *et al.* (JETSCAPE), *Phys. Rev. C* **103**, 054904 (2021), arXiv:2011.01430 [hep-ph].
- [55] G. Nijs, W. van der Schee, U. Gürsoy, and R. Snellings, *Phys. Rev. C* **103**, 054909 (2021), arXiv:2010.15134 [nucl-th].
- [56] J. Auvinen, K. J. Eskola, P. Huovinen, H. Niemi, R. Paatelainen, and P. Petreczky, *Phys. Rev. C* **102**, 044911 (2020), arXiv:2006.12499 [nucl-th].
- [57] J. E. Parkkila, A. Onnerstad, and D. J. Kim, *Phys. Rev. C* **104**, 054904 (2021), arXiv:2106.05019 [hep-ph].
- [58] A. V. Giannini, M. N. Ferreira, M. Hippert, D. D. Chinellato, G. S. Denicol, M. Luzum, J. Noronha, T. Nunes da Silva, and J. Takahashi (ExTrEMe), *Phys. Rev. C* **107**, 044907 (2023), arXiv:2203.17011 [nucl-th].
- [59] M. Luzum and J.-Y. Ollitrault, *Nucl. Phys. A* **904-905**, 377c (2013), arXiv:1210.6010 [nucl-th].
- [60] G. S. Denicol, C. Gale, S. Jeon, J. F. Paquet, and B. Schenke, (2014), arXiv:1406.7792 [nucl-th].
- [61] C. Shen, Z. Qiu, and U. Heinz, *Phys. Rev. C* **92**, 014901 (2015), arXiv:1502.04636 [nucl-th].
- [62] R. S. Bhalerao, A. Jaiswal, and S. Pal, *Phys. Rev. C* **92**, 014903 (2015), arXiv:1503.03862 [nucl-th].
- [63] C. Loizides, *Phys. Rev. C* **94**, 024914 (2016), arXiv:1603.07375 [nucl-ex].
- [64] G. Giacalone, P. Guerrero-Rodríguez, M. Luzum, C. Marquet, and J.-Y. Ollitrault, *Phys. Rev. C* **100**, 024905 (2019), arXiv:1902.07168 [nucl-th].
- [65] F. Gelis, G. Giacalone, P. Guerrero-Rodríguez, C. Marquet, and J.-Y. Ollitrault, (2019), arXiv:1907.10948 [nucl-th].
- [66] P. Carzon, S. Rao, M. Luzum, M. Sievert, and J. Noronha-Hostler, *Phys. Rev. C* **102**, 054905 (2020), arXiv:2007.00780 [nucl-th].
- [67] R. Snyder, M. Byres, S. H. Lim, and J. L. Nagle, *Phys. Rev. C* **103**, 024906 (2021), arXiv:2008.08729 [nucl-th].
- [68] B. G. Zakharov, *JETP Lett.* **112**, 393 (2020), arXiv:2008.07304 [nucl-th].
- [69] J.-B. Rose, J.-F. Paquet, G. S. Denicol, M. Luzum, B. Schenke, S. Jeon, and C. Gale, *Nucl. Phys. A* **931**, 926 (2014), arXiv:1408.0024 [nucl-th].
- [70] S. Plumari, G. L. Guardo, F. Scardina, and V. Greco, *Phys. Rev. C* **92**, 054902 (2015), arXiv:1507.05540 [hep-ph].
- [71] P. Alba, V. Mantovani Sarti, J. Noronha, J. Noronha-Hostler, P. Parotto, I. Portillo Vazquez, and C. Ratti, *Phys. Rev. C* **98**, 034909 (2018), arXiv:1711.05207 [nucl-th].
- [72] A. Majumder, B. Muller, and X.-N. Wang, *Phys. Rev. Lett.* **99**, 192301 (2007), arXiv:hep-ph/0703082.
- [73] P. Staig and E. Shuryak, *Phys. Rev. C* **84**, 034908 (2011), arXiv:1008.3139 [nucl-th].
- [74] S. S. Gubser and A. Yarom, *Nucl. Phys. B* **846**, 469 (2011), arXiv:1012.1314 [hep-th].
- [75] R. A. Lacey, Y. Gu, X. Gong, D. Reynolds, N. N. Ajitanand, J. M. Alexander, A. Mwai, and A. Taranenko, (2013), arXiv:1301.0165 [nucl-ex].
- [76] M. Aaboud *et al.* (ATLAS), *Eur. Phys. J. C* **78**, 997 (2018), arXiv:1808.03951 [nucl-ex].
- [77] S. Acharya *et al.* (ALICE), *JHEP* **07**, 103 (2018), arXiv:1804.02944 [nucl-ex].
- [78] S. Acharya *et al.* (ALICE), *Phys. Lett. B* **784**, 82 (2018), arXiv:1805.01832 [nucl-ex].
- [79] K. Aamodt *et al.* (ALICE), *Phys. Rev. Lett.* **106**, 032301 (2011), arXiv:1012.1657 [nucl-ex].
- [80] J. Adam *et al.* (ALICE), *Phys. Rev. Lett.* **116**, 222302 (2016), arXiv:1512.06104 [nucl-ex].
- [81] S. Acharya *et al.* (ALICE), *Phys. Lett. B* **790**, 35 (2019), arXiv:1805.04432 [nucl-ex].
- [82] A. M. Sirunyan *et al.* (CMS), *Phys. Lett. B* **799**, 135049 (2019), arXiv:1902.03603 [hep-ex].
- [83] M. L. Miller, K. Reygers, S. J. Sanders, and P. Steinberg, *Ann. Rev. Nucl. Part. Sci.* **57**, 205 (2007), arXiv:nucl-ex/0701025.
- [84] B. Alver *et al.* (PHOBOS), *Phys. Rev. Lett.* **98**, 242302 (2007), arXiv:nucl-ex/0610037.
- [85] K. Tsukada *et al.*, *Phys. Rev. Lett.* **118**, 262501 (2017), arXiv:1703.04278 [nucl-ex].